Contract No.:

This manuscript has been authored by Savannah River Nuclear Solutions (SRNS), LLC under Contract No. DE-AC09-08SR22470 with the U.S. Department of Energy (DOE) Office of Environmental Management (EM).

Simulation of hydrogen adsorption systems adopting the flow through cooling concept

Claudio Corgnale[1*], Bruce Hardy[1], Richard Chahine[2], Daniel Cossement[2], David Tamburello[1], Donald Anton[1]

1 Savannah River National Laboratory, Aiken, SC 29808, USA

2 Hydrogen Research Institute, Université du Québec à Trois-Rivières, Trois-Rivières, QC, Canada. G9A 5H7

ABSTRACT

Hydrogen storage systems based on adsorbent materials have the potential of achieving the U.S. Department of Energy (DOE) targets, especially in terms of gravimetric capacity. This paper deals with analysis of adsorption storage systems adopting the flow through cooling concept. By this approach the feeding hydrogen provides the needed cold to maintain the tank at low temperatures. Two adsorption systems have been examined and modeled adopting the Dubinin-Astakhov model, to see their performance under selected operating conditions. A first case has been analyzed, modeling a storage tank filled with carbon based material (namely MaxSorb®) and comparing the numerical outcomes with the available experimental results for a 2.5 L tank. Under selected operating conditions (minimum inlet hydrogen temperature of approximately 100 K and maximum pressure on the order of 8.5 MPa) and adopting the flow through cooling concept the material shows a gravimetric capacity of about 5.7 %. A second case has been modeled, examining the same tank filled with metal organic framework material (MOF5®) under approximately the same conditions. The model shows that the latter material can achieve a (material) gravimetric capacity on the order of 11%, making the system potentially able to achieve the DOE 2017 target.

Nomenclature

c = Molar concentration of H_2 (mol/m^3)

$C_{P\ Ads}$ = Specific heat of adsorbent (J/kg-K)

DOE = US Department Of Energy

* Corresponding author Tel: 8036179689

E_a = Characteristic free energy of adsorption from the Dubinin-Astakhov model (J/mol). $\equiv \alpha + \beta T$

h = Molar enthalpy of the gas (J/mol)

HSECoE = Hydrogen Storage Engineering Center of Excellence

$\underline{\underline{I}}$ = 2nd order identity tensor

k = Thermal conductivity (W/(m-K))

M_{H2} = Molecular weight of hydrogen (0.002016 kg/g-mol)

n_a = Absolute adsorption (mol of H_2/kg of adsorbent)

n_{ex} = Adsorbed hydrogen excess, compared to gaseous state hydrogen (mol of H_2/kg of adsorbent)

n_{max} = Limiting adsorption, associated with the maximum hydrogen loading of the entire adsorption volume (mol of H_2/(kg of adsorbent))

n_{total} = Total hydrogen stored in the bed (mol of H_2/(kg of adsorbent))

P = Pressure (Pa)

P_0 = Pseudo-pressure for Dubinin-Astakhov model (Pa)

R = Gas constant = 8.314 J/(mol-K)

S_0 = Mass source of hydrogen per unit of total volume (kg/m^3-s)

SLPM = Standard liter per minute

SRNL = Savannah River National Laboratory

T = Temperature (K)

u_0= Molar internal energy of free gas at the system temperature T and a pressure of 1 atm (J/mol)

UQTR = University du Québec à Trois Rivières

V_a = Adsorbed volume per mass of adsorbent (m^3/(kg of adsorbent)). The void volume within the adsorbent for which the gas concentration exceeds that given by the equation of state, per mass of adsorbent.

V_v = Void volume per mass of adsorbent (m^3/(kg of adsorbent)), measured by He filling.

$\vec{v}$ = Mean interstitial gas velocity vector (m/s) or velocity of gas (m/s)

$\vec{v}_s$ = Superficial velocity vector (m/s)

W_p = Compression/Expansion work related power (W/m^3)

W_a = Adsorption/Desorption heat related power (W/m^3)

Z = Hydrogen compressibility factor.

Greek

α = Enthalpic contribution to the characteristic free energy of adsorption, E_a, (J/mol)

β = Entropic contribution to the characteristic free energy of adsorption, E_a, (J/mol-K)

ε = Effective porosity, volume available for flow = $\rho_{Carbon}(V_v - V_a)$

ΔU_a = Internal energy per mass of adsorbent of the condensed phase of the gas at a temperature T and pressure P relative to free gas at a temperature T and a pressure of 1 atm (J/kg)

η_d = Dilatational viscosity of hydrogen (Pa-s) = 0 Pa-s in this analysis

κ = Bed permeability (m^2)

μ = Dynamic viscosity of hydrogen (Pa-s)

ρ = Mass density of hydrogen (kg/m^3)

ρ_{Ads} = Bulk mass density of adsorbent (kg/m^3)

$\underline{\underline{\tau}}$ = Fluid stress tensor (Pa)

1. INTRODUCTION

Onboard hydrogen storage is one of the main technical hurdles to be overcome to make hydrogen driven vehicles a practical possibility. To increase the energy density of the hydrogen stored onboard three realistic options are available today. Hydrogen can be compressed at high pressures, or can be liquefied, or it can be stored by forming chemical or physical bonds with other materials. The first two possibilities require either very high pressure (on the order of 350-700 bar for compressed hydrogen storage) or very low temperatures (on the order of 20-30 K for liquefied hydrogen storage)(1). This implies that a series of issues needs solving to make such two options effective systems to store hydrogen. For instance, the high pressure compressed hydrogen storage requires noticeable compression work and feasible materials to work at such conditions. Liquid hydrogen storage requires a great amount of compression work that makes the technique particularly expensive in terms of lifetime costs. The third storage option, which sees the adoption of materials that bond with hydrogen is particularly attractive. This system shows different positive aspects, such as low operating pressures (lower than compressed hydrogen case) and temperatures in general higher than the liquid hydrogen temperature. Among the various potential materials to store hydrogen onboard, metal hydrides and adsorbents are among

the most attractive ones. However metal hydrides show a low gravimetric capacity (2) (3) compared to the DOE targets (4): a material with gravimetric capacity at least on the order of 11% or higher is needed to achieve the 2017 DOE target (3). Using materials which adsorb hydrogen by physisorption, the hydrogen weight fraction can be noticeably increased, making such materials potentially capable to attain the values given by the 2017 DOE target. However, due to the nature of their physical bonds (5)(6)(7)(8) , hydrogen needs storing at low temperatures (in general on the order of liquid nitrogen temperature) to achieve a high H_2 capacity. One of the techniques already investigated to keep the storage tank temperature down to such values consists in having a liquid nitrogen bath surrounding the wall of the hydrogen storage tank (9). The work presented in the paper focuses on a new approach, referred to as the 'flow through cooling' concept with the feeding hydrogen providing the necessary cold to keep the adsorbent at low temperature. The paper reports the results of the activities carried out at SRNL, in conjunction with UQTR, as part of the DOE's HSECoE work on the flow through cooling concept. Numerical simulation results shall be presented and compared to the experimental data available from UQTR facility tests for carbon based materials (namely MaxSorb®). In addition to that, numerical simulation results shall be presented about a Metal Organic Framekork material (MOF5®) as well, comparing its performance with that of the carbon based material.

2. EXPERIMENTAL TESTS

A picture of the UQTR experimental test bench is reported in Figure 1.

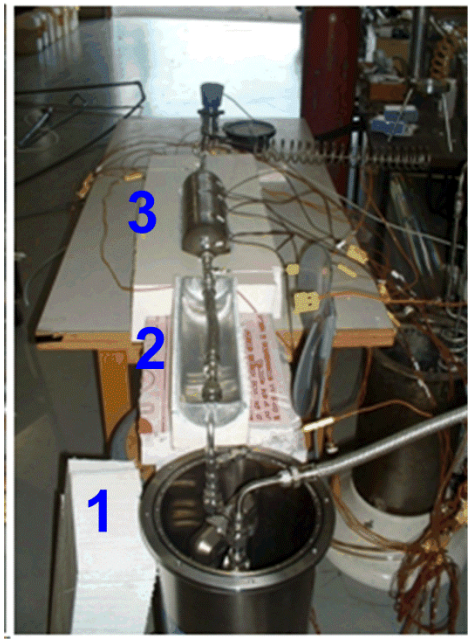

Figure 1: Overview of the UQTR test bench (1: First heat exchanger to cool the feeding hydrogen – 2: Second heat exchanger – 3: Hydrogen storage reservoir)

The gas passes through a two loops U-tube type heat exchanger with tube diameter of 0.025 m, filled with stainless steel balls (0.0024 m diameter) and immersed in a liquid nitrogen bath (1 in Figure 1). A thermocouple monitors the temperature directly after the heat exchanger. During the test, the connection duct between the heat exchanger and the reservoir (2 in Figure 1) is also immersed in liquid nitrogen to keep the gas at low temperature with a second thermocouple checking the gas temperature before feeding the reservoir (3 in Figure 1). The tank is similar to that described in the Reference (9), with a volume of 2.5 L (0.0025 m^3) and a mass of MaxSorb® material of 0.671 kg packed inside the tank. The geometry of the reservoir will be described with a few more details in the next sections of the paper. A third thermocouple is placed at the exit of the reservoir to measure the exit gas temperature. The recirculating hydrogen which leaves the bed, without adsorbing in that, is heated through a second heat exchanger, and it flows through a pressure gauge and a back pressure regulator, which fixes the pressure inside the reservoir. By this system the gas leaving the reservoir is heated up, before further measurements by components which are sensitive to low temperatures. Six thermocouples are placed inside the reservoir along the central axis and eight additional thermocouples are placed on the external surface of the tank to have the values of the boundary temperatures to be used in the numerical system model.

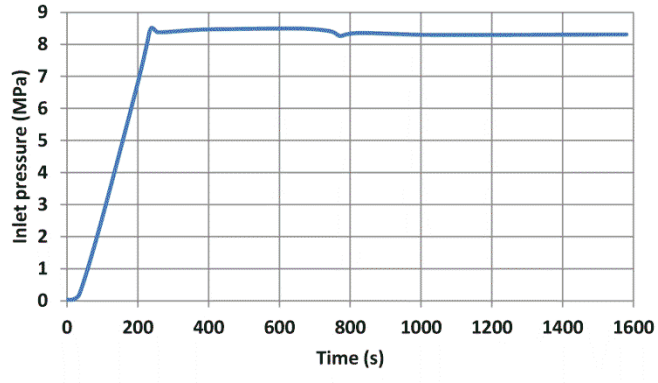

Figure 2: Pressure profile of inlet hydrogen during the charging time of UQTR experiments with MaxSorb® adsorbent

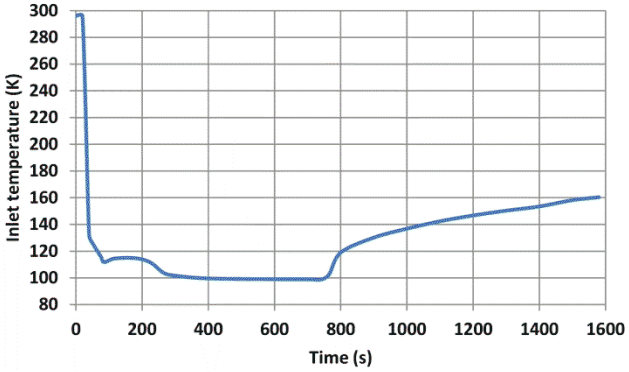

Figure 3: Temperature profile of inlet hydrogen during the charging time of UQTR experiments with MaxSorb® adsorbent

The experiments were carried out under temperature and pressure conditions reported at Figure 2 and Figure 3. The feeding hydrogen pressure profile is reported in Figure 2 during the charging time, with the back pressure regulator fixing the maximum pressure at values on the order of 8.5 MPa inside the bed. The feeding hydrogen temperature profiles are reported in Figure 3, with the minimum temperature of the inlet hydrogen of approximately 100 K, achieved in the time period from approximately 250 s to 770 s.

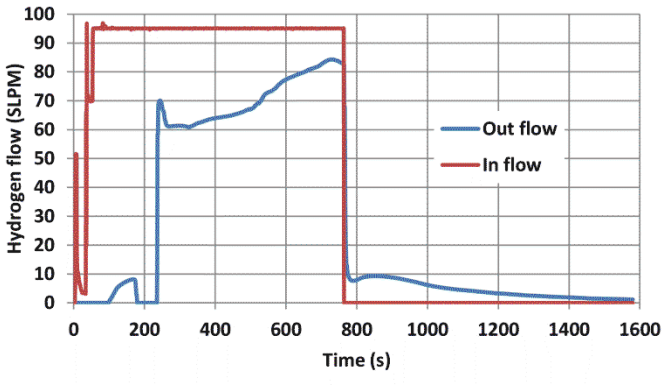

Figure 4: Inlet and outlet hydrogen flow rates in SLPM

The inlet and outlet hydrogen flow rates are reported in Figure 4 with the maximum inlet hydrogen flow equal to 95 SLPM.

The boundary conditions adopted in the numerical model (inlet pressure, inlet temperature and outlet velocity) have been established according to the profiles reported at Figures 2-4.

1. NUMERICAL MODEL

The detailed model adopted to simulate the system is based on mass, momentum and energy balance equations, with additional ancillary equations to evaluate the thermodynamic properties of the adsorption process and the hydrogen gas state.

1.1. Mass, momentum and energy balance equations

The differential equation of the mass balance for hydrogen in gaseous state in the adsorbent porous material is reported at Equation 1:

$$\varepsilon \frac{\partial \rho}{\partial t} + \nabla \cdot \left(\rho \vec{v}_s \right) = S_0 \qquad (1)$$

with $\vec{v}_s = \varepsilon \vec{v}$ being the superficial gas velocity and

$$S_0 = -M_{H2}\rho_{Ads}\frac{\partial n_a}{\partial t} \tag{2}$$

The mass balance equation of hydrogen flowing in a free volume without porous media and without mass sources has the usual expression:

$$\frac{\partial \rho}{\partial \mathrm{t}} + \nabla \cdot \left(\rho \vec{\mathrm{v}}\right) = 0 \tag{3}$$

The differential form of momentum balance equation (Brinkman equation) for hydrogen flowing inside the porous media under laminar flow conditions is reported at Equation 4:

$$\begin{aligned} &\frac{\rho}{\varepsilon}\frac{\partial \vec{v}_s}{\partial t} + \left(\frac{\mu}{\kappa} + \frac{S_0}{\varepsilon^2}\right)\vec{v}_s = \\ &-\nabla P + \nabla \cdot \left[\frac{\mu}{\varepsilon}\left(\nabla \vec{v}_s + \nabla \vec{v}_s{}^T\right)\right] - \nabla \cdot \left[\left(\frac{2\mu}{3} - \eta_d\right)\left(\frac{1}{\varepsilon}\right)\left(\nabla \cdot \vec{v}_s\right)\underline{\underline{I}}\right] \end{aligned} \tag{4}$$

This equation also includes the viscous stress term expressed in terms of velocity components, taking into account the viscosity of the media as well.

For free flows without porous media (such as in connecting tubes and open channels in the tank) the momentum balance equation under laminar conditions is expressed as:

$$\rho\frac{D\vec{v}}{Dt} = -\nabla P - \nabla \cdot \underline{\underline{\tau}} \tag{5}$$

Energy balance of the adsorbent system, comprising the condensed phase mixture (i.e. carbon material and adsorbed hydrogen) and the hydrogen in gaseous state, is reported at Equation 6:

$$\begin{aligned} &\varepsilon c\frac{\partial h}{\partial T}\frac{\partial T}{\partial t} - \nabla \cdot k\nabla T \\ &= -c\frac{\partial h}{\partial T}\vec{v}_s \cdot \nabla T \underbrace{- \frac{T}{c}\frac{\partial c}{\partial T}\left(\varepsilon\frac{\partial P}{\partial t} + \vec{v}_s \cdot \nabla P\right)}_{\text{Pressure work}} + \underbrace{\frac{\mu}{\varepsilon}\left[\left(\nabla \vec{v}_s + \nabla^T \vec{v}_s\right) - \left(\frac{2}{3} - \eta_d\right)\nabla \cdot \vec{v}_s \underline{\underline{I}}\right] : \nabla \vec{v}_s}_{\text{Viscous dissipation}} \\ &- \frac{hS_0}{M_{H2}} - \rho_{Ads}\left(\underbrace{\frac{\partial \Delta U_a}{\partial t} + \frac{\partial\left(u_0 n_a\right)}{\partial t}}_{\text{Sorption Energy}} + C_{P\ Ads}\frac{\partial T}{\partial t}\right) \end{aligned} \tag{6}$$

Equation 6 is the general energy balance equation in a porous medium reacting with a fluid. It accounts for pressure work term and viscous dissipation term, yet the terms related to the kinetics energy and to gravitational force work are neglected. The 'Sorption Energy' term accounts for the time variation of total internal energy of the adsorbed hydrogen due to adsorption reaction. To evaluate this term, the numerical model needs to be completed by adding two further relationships assessing ΔU_a and n_a. The relative internal energy term (ΔU_a) can be expressed by using the Dubinin-Astakhov (DA) model (5) (6):

$$\Delta U_a = -\frac{n_{\max}\alpha\sqrt{\pi}}{2}\left[1 - erf\left(\sqrt{-\ln\left(\frac{n_a}{n_{\max}}\right)}\right)\right] + n_a\left[RT - \alpha\sqrt{-\ln\left(\frac{n_a}{n_{\max}}\right)}\right] \quad (7)$$

Likewise, the amount of hydrogen adsorbed (n_a) can be evaluated by using the DA model (5) (6):

$$n_a = n_{\max}\exp\left[-\left(\frac{RT}{E_a}\right)^2 \ln^2\left(\frac{P_0}{P}\right)\right] \quad (8)$$

with: $E_a = \alpha + \beta T$

The amount of hydrogen adsorbed (n_a) contributes into the total amount of hydrogen stored inside the bed, as reported at Equation 9:

$$n_{total} = n_a + c\left(V_v - V_a\right) \quad (9)$$

The total amount of hydrogen stored in the bed is given by the hydrogen adsorbed in the material and the hydrogen stored as gas at high pressure and low temperature.

Another significant parameter (n_{ex}) can be defined, which represents the additional amount of hydrogen stored by adsorption, compared to the gaseous hydrogen occupying the same space:

$$n_{ex} = n_a - cV_a \quad (10)$$

By using the previous equations, the bed void fraction value can be estimated by the following relationship:

$$\varepsilon \equiv \rho_{Ads}\left(V_v - V_a\right) \quad (11)$$

For hydrogen flowing into no porous volumes, the energy balance equation is reported at Equation 12:

$$c\frac{\partial h}{\partial T}\frac{\partial T}{\partial t} - \nabla\cdot k\nabla T = -c\frac{\partial h}{\partial T}\vec{v}\cdot\nabla T - \frac{T}{c}\frac{\partial c}{\partial T}\left(\frac{\partial P}{\partial t} + \vec{v}\cdot\nabla P\right) - \underline{\underline{\tau}} : \nabla\vec{v} \quad (12)$$

The DA model parameter values for powder MaxSorb® (as used in the experiments carried out at UQTR) are reported at Table 1 and are available from References (5)(6). Table 2 shows the correspondent parameters for powder non-compacted MOF5®. Such values have been assessed at SRNL, in conjunction with Ford, within the HSECoE and validated against experimental data available from Ford (10).

Table 1: Model parameters for MaxSorb®

n_{max} [mol/kg of adsorbent]	71.6
P_0 [MPa]	1470
α [J/mol]	3080
β [J/mol K]	18.9
V_a [m^3/(kg of adsorbent)]	0.00143
V_v [m^3/(kg of adsorbent)]	0.0029

Table 2: Model parameters for MOF5®

n_{max} [mol/kg of adsorbent]	96.4
P_0 [MPa]	1387
α [J/mol]	2985
β [J/mol K]	15.3
V_a [m^3/(kg of adsorbent)]	0.0017
V_v [m^3/(kg of adsorbent)]	0.00725

The model evaluates the hydrogen state adopting Equation 13, with compressibility factor which modifies the ideal gas state equation:

$$P = Z(P,T)\rho RT \qquad (13)$$

The compressibility factor has been evaluated by the polynomial expression reported at Reference (9). In addition to that, the hydrogen specific heat, enthalpy, thermal conductivity and viscosity have been evaluated by polynomial relationships function of pressure and temperature as well, as reported at Reference (9). The properties of the adsorbent materials have been evaluated according to Reference ((9)). The specific heat has been evaluated adopting a cubic spline to interpolate the values of the expression from Reference (11) and included in the model. Due to the lack of data, the same expression was used for MOF5® material as well, based on Reference (9). The adsorbent material bulk density has been assumed equal to 300 kg/m^3 for MaxSorb® ((6)), and equal to 130 kg/m^3 for MOF5®, based on the data available from Ford (10). The bed thermal conductivity (accounting for adsorbent material and hydrogen) has been assumed equal to 0.1 W/mK for both materials, based on recent experiments and evaluations carried out within the HSECoE by General Motors and Ford.

3.2 Model geometry and conditions

The reservoir model geometry has been set up according to the size and the characteristics of the experimental device available at UQTR and briefly described above. A 2D axial symmetric geometry has been adopted to model the actual experimental device. This results in a strong reduction of the computing time with a good approximation of the actual device geometry. A sketch is reported in Figure 5, comprising the following regions: 1) the inlet hydrogen duct, 2) the axial thermocouple region (TC1-TC6) to measure the adsorption temperature profiles, 3) the outlet hydrogen section, 4) the reservoir wall, 5) the adsorbent material.

The cylinder external radius (including thermocouples TC1-TC6 region and wall region) is 0.05 m, while the length of the reservoir, including the domes of the tank, is 0.422 m. The inlet tube length is 0.15 m, with an internal radius of 0.00386 m. The six thermocouples (TC1-TC6) have been placed in a cylindrical tube, and spaced 0.045 m. The numerical model geometry includes a hydrogen filter inside the reservoir, connected to the inlet tube and welded to a thin dish, according to the experimental device configuration. The dish is placed inside the reservoir to purify the feeding hydrogen and to prevent the inlet hydrogen to flow directly to the first thermocouple. This allows the TC1 measurement to be less affected by the inlet hydrogen temperature and more related to the temperature variation due to the hydrogen adsorption process.

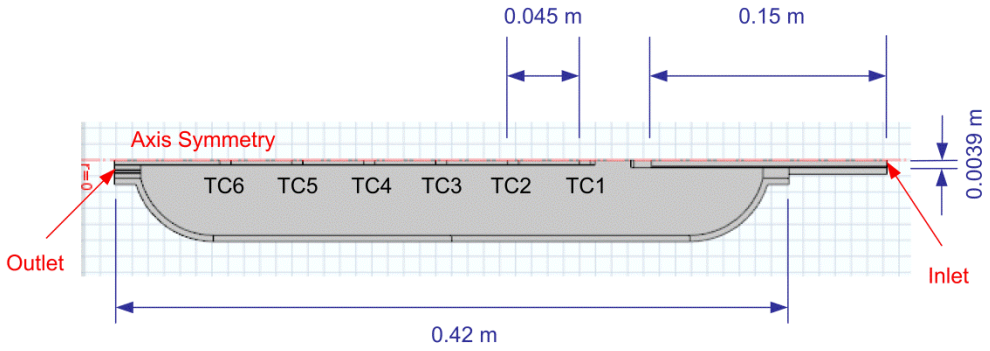

Figure 5: Reservoir geometry for the numerical simulation

Mass, momentum and energy conservation equations have been integrated by COMSOL Multiphysics® Finite Element software, with the boundary and initial conditions described in the following sections and based on the experimental conditions. The initial temperature of the overall system has been assumed equal to 298 K, with initial bed pressure of 0.035 MPa and null velocity inside the bed. The profiles of the inlet hydrogen pressure and temperature are shown in Figure 2 and 3 respectively. The outlet hydrogen velocity has been assessed (to integrate the momentum equation) according to the experimental data available for the outlet hydrogen flow rate from experiments carried out at UQTR and reported in Figure 4. Adiabatic boundary

condition has also been assumed for the outlet section and for the overall system wall to integrate the energy conservation equation[†].

The thermo-physical properties of the thermocouples region and the reservoir wall, in terms of specific heat, thermal conductivity, density of the material, can be found at Reference (9). The specific heat and thermal conductivity of the material (SS316) composing the reservoir and tube walls have been modeled by adopting a polynomial expression fitting NIST data (9). The properties of MgO powder, which is the material filling the thermocouple supporting tube, have been included in the model, based on the crystal MgO properties and suitably modifying it, following the approach described in Reference (9).

2. RESULTS

2.1. MaxSorb® numerical and experimental results

Temperature profiles obtained from numerical simulation are reported in Figures 6-8 showing a comparison between numerical and experimental values of TC1, TC2 and TC4. The temperature profiles measured by the other thermocouples (not reported in the document) are similar to the TC4 profile with similar differences between experimental and numerical data.

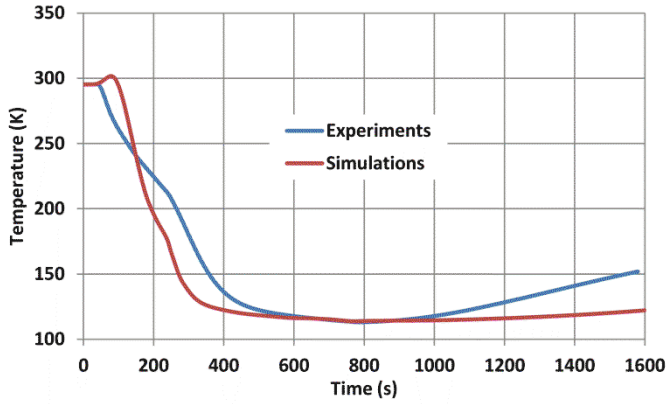

Figure 6: Numerical and experimental profiles of TC1 temperature during charging time for MaxSorb® material

The numerical results, in general, are in agreement with the corresponding experimental values. The TC4 minimum temperature value is achieved at about 800 s, with a maximum difference of approximately 7% between experimental and numerical values. The maximum temperature predicted by the model during the experiments (for TC4) is in agreement with that obtained from the experimental tests, with a difference of about 3% between the two values. The most relevant differences between the model and the experimental results can be observed for TC1 after

[†] Other simulations have been carried out assuming air convective heat transfer as wall boundary condition (heat transfer coefficient equal to 10 W/m^{2}K) and not relevant variations have been noticed

opening the back pressure valve. A maximum temperature difference of approximately 30 K between numerical and experimental results is observed at 1600 s. This is likely due to the fact that the properties (specific heat and thermal conductivity in particular) of carbon material are not constant inside the bed and are most likely affected by temperature and stored hydrogen amount as well. In addition to that, adopting a more detailed geometry (3D geometry) would likely result in more accurate predictions of the experimental results.

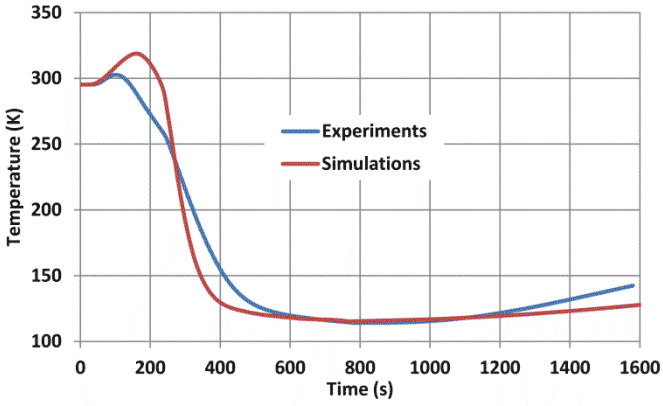

Figure 7: Numerical and experimental profiles of TC2 temperature during charging time for MaxSorb® material

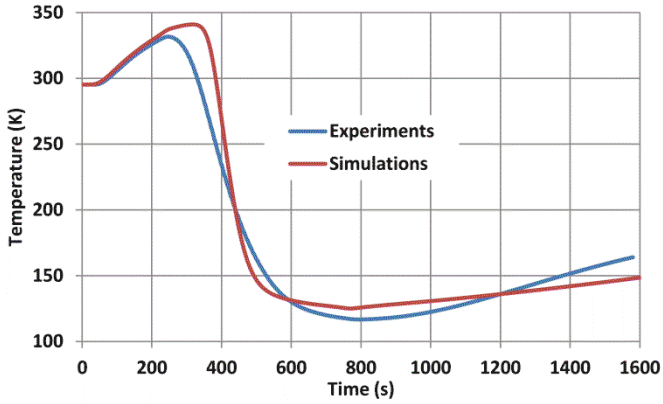

Figure 8: Numerical and experimental profiles of TC4 temperature during charging time for MaxSorb® material

The model well describes the temperature increase during the first period of the charging process, especially for TC4. This is a combined effect of the pressure work and adsorption heat, included in the energy balance equation of the numerical model.

The compression/expansion power term, as included in the energy balance equation (Equation 6) (W_p) is:

$$W_p = -\frac{T}{c}\frac{\partial c}{\partial T}\left(\varepsilon\frac{\partial P}{\partial t} + \vec{v}_s \cdot \nabla P\right) \quad (14)$$

The adsorption/desorption power term (W_a) is:

$$W_a = -\rho_{Ads}\left(\frac{\partial \Delta U_a}{\partial t} + \frac{\partial (u_0 n_a)}{\partial t}\right) \quad (15)$$

The profiles of both terms[‡] are shown in Figure 9, plotting (on y axis) the pressure work-related power term (W_p), and the adsorption heat-related adsorption power (W_a), with charging time on x axis. Three different sections can be identified during charging. In the first part (from 0 to approximately 250 s) the pressure variation plays an important role, resulting in positive values of the correspondent term. During the same charging time, the adsorption power values are negative. This is due to the fact that at the beginning of the charging process, with low (or null) amount of hydrogen stored, the term $\frac{\partial (u_0 n_a)}{\partial t}$ is positive and prevails on the absolute value of the negative value term $\frac{\partial \Delta U_a}{\partial t}$. The influence of W_p on the overall energy balance cannot be neglected, being on the same order of magnitude of the W_a term. In the second part of the profiles reported in Figure 9, from approximately 250 s to about 770 s, the contribution of W_p term is approximately null, since a fixed pressure value of approximately 8.5 MPa is maintained inside the bed. Given the increased amount of hydrogen adsorbed and the decrease of temperature, the adsorption power values become positive with the absolute value of the term $\frac{\partial \Delta U_a}{\partial t}$, being higher than $\frac{\partial (u_0 n_a)}{\partial t}$. In the last part of the charging process up to 1600 s, when hydrogen does not feed the reservoir anymore, pressure is still maintained approximately at the same values. Thus the only contribution to the energy balance is given by the adsorption power term. Due to the increase of temperature, a (little) desorption process can be observed for the last part of the experiments.

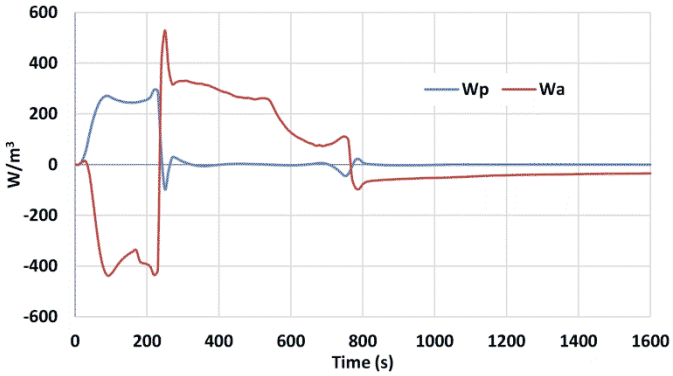

[‡] The plotted terms are the average value of the Equations 14 and 15 on the adsorbent domain

Figure 9: Modeling results for W_p (pressure work-related power) and W_a (adsorption heat-related power), during charging of MaxSorb® material

The storage reservoir capacity is shown in Figure 10. The figure shows the profiles of the total specific (per kg of adsorbent) amount of hydrogen stored (n_{total}), the specific amount of hydrogen adsorbed in the material (n_a) and the specific excess of hydrogen stored in solid form. The maximum amount of hydrogen stored in the bed is reached at approximately 800 s with a weight fraction capacity of about 5.7%. To attain this value, the ratio between the inlet mass of hydrogen feeding the reservoir (approximately 0.103 kg) and the total mass of hydrogen stored in the bed (approximately 0.0382 kg) needs to be about 2.7. Hydrogen adsorbed in solid state represents approximately 70% of the total hydrogen stored, resulting in a weight fraction of approximately 4%. The remainder weight fraction (1.7%) is due to the hydrogen stored under gaseous state at low temperature. The maximum excess adsorption achieved in the charging process gives a weight capacity of approximately 2.4%.

The results have been obtained with a minimum temperature of approximately 115 K and maximum pressure on the order of 8.5 MPa achieved inside the bed during the charging process. Further analyses will be carried out in the future, designing the heat exchangers to achieve a minimum temperature on the order of that of liquid nitrogen at ambient pressure (77 K). Under these conditions a weight fraction capacity on the order of 7% is expected to be achieved, based on Equations 8 and 9. In addition, the inlet hydrogen pressure is being planned to increase up to about 100-200 bar in the future analyses, resulting in an even higher weight fraction capacity.

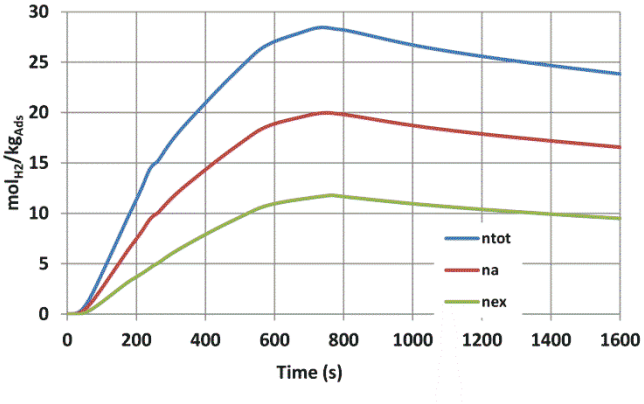

Figure 10: Hydrogen adsorbed (total hydrogen, adsorbed hydrogen and excess hydrogen adsorbed) for MaxSorb®

2.2. Performance comparison between MaxSorb® and MOF5®

Additional analyses have been carried out to evaluate MOF5® material performance and compare it with MaxSorb®. The same vessel geometry has been utilized, adopting the same conditions as for the carbon material case. Inlet temperature and pressure profiles are as those reported at

Figure 2 and Figure 3. The outlet velocity has been assessed based on the flow rate profiles reported in Figure 4. The maximum pressure is equal to about 8 MPa for MOF5® case, and the minimum temperature is equal to approximately 100 K. The same outlet conditions have been assumed as previously described for MaxSorb® material.

Results are reported in the following figures and compared to the MaxSorb® corresponding data. Figure 11 shows the results obtained from numerical simulations, plotting the profiles of the amount of hydrogen stored (n_a, n_{ex}, n_{total}), accounting for the hydrogen stored as compressed gas as well. The maximum specific total amount of hydrogen stored by MOF5® is approximately 89% larger than the corresponding MaxSorb® value, reaching a total gravimetric (material) capacity of almost 11%. The ratio between the total mass of inlet hydrogen feeding the reservoir and the total amount of hydrogen adsorbed is equal to approximately 3.1 (i.e. approximately 15% higher than MaxSorb® case). The difference between the adsorption capacities of the two materials is mainly due to the amount of compressed hydrogen stored inside the void space, which represents almost 61% of the total hydrogen for MOF5®, and only 30% for MaxSorb®. This is caused by the fact that the void space available in the MOF5® material (ε=0.722) is almost 64% higher than the correspondent MaxSorb® value (ε=0.441). The profiles of the specific amount of adsorbed hydrogen (n_a and n_{ex}) reported in Figure 11 show similar capacities for MaxSorb® and MOF5® materials. However during the initial charging period (up to approximately 400 s) the MOF5® specific hydrogen adsorbed (n_a) is lower than MaxSorb®, with a maximum difference of n_{ex} between the two materials of approximately 46% at about 100 s. This is due to the fact that a large quantity of hydrogen is stored inside MOF5® material as compressed gas, especially at the beginning of the charging process, when the compression work plays an important role. Consequently MOF5® n_{ex} values are lower than MaxSorb® values especially at the beginning of the process. The results reported in Figure 12, which show the average temperatures inside the two adsorbents, also highlight this aspect. The maximum and minimum average temperatures achieved inside the bed are approximately the same for the two adsorbents with a difference of 5 K for the minimum temperatures (163 K for MOF5® and 168 K for MaxSorb®). The main difference between the two materials is related to the first part of the adsorption process, up to about 500 s, when the temperature inside MOF5® is lower than MaxSorb® values reaching a maximum difference of approximately 30 K. The power released during the MOF5® adsorption process, given by the integration of the W_a term on the overall adsorbent volume, is significantly lower than the MaxSorb® material, since the hydrogen adsorbed per volume is lower than MaxSorb®. This is mainly due to the adsorbent material density difference, which also results in having the amount of hydrogen stored as compressed gas inside the MOF5® material larger than MaxSorb®. In addition to that, the hydrogen recirculation for MOF5® system is higher than that needed for MaxSorb® system. This also contributes to reduce the temperature of the MOF5® adsorbent system in comparison with MaxSorb®.

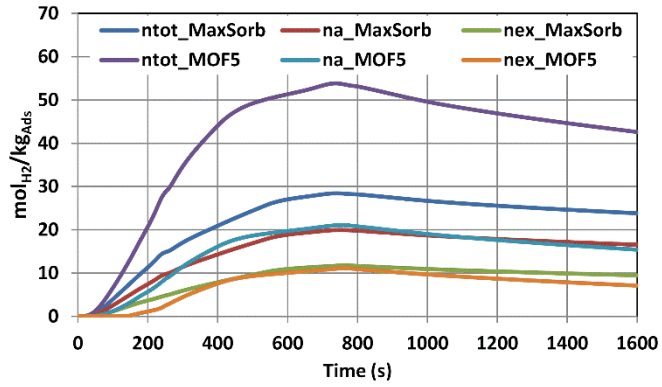

Figure 11: Hydrogen adsorbed (total hydrogen, adsorbed hydrogen and excess hydrogen adsorbed) for MaxSorb® and MOF5® materials

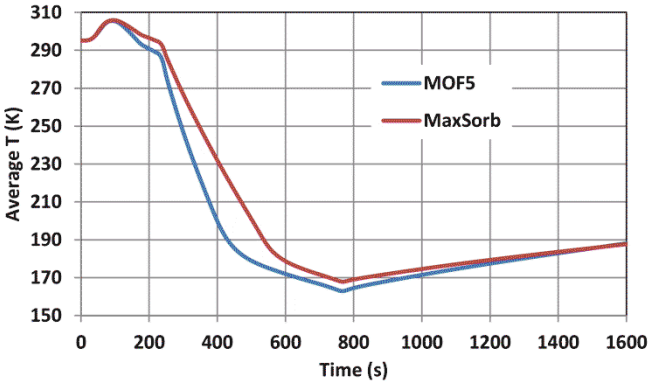

Figure 12: Average bed temperature during charging time for MaxSorb® and MOF5® materials

3. Summary and conclusions

A hydrogen adsorbent system, based on carbon material (namely MaxSorb®), has been simulated by the Finite Element COMSOL® software, adopting a new cooling method, referred to as 'flowthrough cooling'. The approach sees the inlet hydrogen itself providing the necessary cold to keep the medium at low temperatures, with no need for other cooling systems (e.g. liquid nitrogen baths). After a description of the model adopted, which accounts for mass, energy and momentum balance, the results have been presented. The operating conditions and the geometrical properties were assumed based on the experiments carried out with the UQTR device. Results obtained from the simulations have also been compared with experimental results available from the UQTR reservoir. The model well described the behavior of the system, giving results in generally good agreement with the experimental ones. Useful information on possible system improvements has also been highlighted. In particular the carbon material-filled system

showed a maximum weight capacity of approximately 5.7% achieved at a pressure of approximately 8.5 MPa and a minimum temperature inside the reservoir of about 110 K. Additional modeling activity has been carried out for the same reservoir filled with metal organic framework (MOF5®) material working under approximately the same operating conditions. The performance of the MOF5®-filled storage system has been evaluated and compared with the carbon material system. The metal organic framework material shows a higher gravimetric capacity (approximately 11%) than MaxSorb® material (approximately 5.7%), mainly due to the increased void space available in the MOF5® material (64% higher than that for MaxSorb®). This makes the metal organic framework material potentially capable to meet the DOE 2017 gravimetric capacity targets. In addition to that, further weight fraction increases can be achieved increasing the operating pressure as well as decreasing the working temperature.

Acknowledgements

This work was performed as part of the US DOE's Hydrogen Storage Engineering Center of Excellence. Dr. Ned Stetson is the DOE manager and his help and direction have really been appreciated.

References

1. Gardiner M. Energy requirements for hydrogen gas compression and liquefaction as related to vehicle storage needs. DOE Hydrogen Program Record, Record # 9013, (2009).

2. Corgnale C, Hardy BJ, Tamburello DA, Garrison SL, Anton DL. Acceptability envelope for metal hydride-based hydrogen storage systems. Int J Hydrogen Energy 2012;37:2812-24.

3. Pasini JM, Corgnale C, van Hassel B, Motyka T, Kumar S, Simmons K. Metal hydride material requirements for automotive hydrogen storage systems. Int J Hydrogen Energy 2013;38:9755-9765.

4. US DOE Targets for Onboard Hydrogen Storage Systems for Light-Duty Vehicles. Available at http://www1.eere.energy.gov/hydrogenandfuelcells/storage/pdfs/targets_onboard_hydro_storage.pdf.

5. Richard M-A, Benard P, Chahine R. Gas adsorption process in activated carbon over a wide temperature range above the critical point. Part 1: modified Dubinin-Astakhov model. Adsorption 2009;15:43-51.

6. Richard M-A, Benard P, Chahine R. Gas adsorption process in activated carbon over a wide temperature range above the critical point. Part 2: conservation of mass and energy. Adsorption 2009;15:53-63.

7. Talu O, Myers A. Molecular simulation of adsorption: Gibbs dividing surface and comparison with experiments. AIChE Journal 2001;47(5):1160-1168.

8. Bhatia S, Myers A. Optimum conditions fro adsorptive storage. Langmuir 2006;22(4):1688-1700.

9. Hardy B, Corgnale C, Chahine R, Richard M-A, Garrison S, Tamburello D, et al. Modeling of adsorbent based hydrogen storage systems. Int J Hydrogen Energy 2012;37:5691-5705.

10. Sudik A. Personal communications. Ford, 2011.

11. Pyda M, Bartkowiak M, Wunderlich B. Computation of heat capacities of solids using a general Tarasov equation. J Thermal Analysis 2009;52(2):631-656.